Calculate the CMB power spectrum: Cosmology II

Johan Mylius Kroken[1,2]

[1] Institute of Theoretical Astrophysics (ITA), University of Oslo, Norway
[2] Center for Computing in Science Education (CCSE), University of Oslo, Norway

May 1, 2023 - GitHub repository link: https://github.com/Johanmkr/AST5220/tree/main/project

ABSTRACT

SOME ABSTRACT

Contents

Nomenclature

Constants of nature

m_e - Mass of electron.
$m_e = 9.10938356 \cdot 10^{-31}$ kg.
$m_{\rm H}$ - Mass of hydrogen atom.
$m_{\rm H} = 1.6735575 \cdot 10^{-27}$ kg.
G - Gravitational constant.
$G = 6.67430 \cdot 10^{-11}$ m^3 kg^{-1} s^{-2}.
k_B - Boltzmann constant.
$k_B = 1.38064852 \cdot 10^{-23}$ m^2 kg s^{-2} K^{-1}.
$\hbar$ - Reduced Planck constant.
$\hbar = 1.054571817 \cdot 10^{-34}$ J s^{-1}.
c - Speed of light in vacuum.
$c = 2.99792458 \cdot 10^{8}$ m s^{-1}.
σ_T - Thomson cross section.
$\sigma_T = 6.6524587158 \cdot 10^{-29}$ m^2.
α - Fine structure constant.
$\alpha = \frac{m_e c}{\hbar}\sqrt{\frac{3\sigma_T}{8\pi}}$

Cosmological parameters

$G_{\mu\nu}$ - Einstein tensor.
$T_{\mu\nu}$ - Stress-energy tensor.
H - Hubble parameter.
$\mathcal{H}$ - Conformal Hubble parameter.
$T_{\rm CMB0}$ - Temperature of CMB today.
a - Scale factor.
x - Logarithm of scale factor.
t - Cosmic time.
z - Redshift.
η - Conformal time.
χ - Co-moving distance.
p - Pressure.
ρ - Density.
r - Radial distance.
d_A - Angular diameter distance.
d_L - Luminosity distance.

---

n_e - Electron density.
n_b - Baryon density.
X_e - Free electron fraction.
τ - Optical depth.
$\tilde{g}$ - Visibility function.

s - Sound horizon.
r_s - Sound horizon at decoupling.
c_s - Wave propagation speed.

Ψ - Newtonian potential perturbation to the metric.
Φ - Spatial curvature perturbation to the metric.
P^μ - Comoving momentum four vector.
$\mathcal{P}_l$ - Legendre polynomial of order l.
k - Fourier mode $k = \mathbf{k}$ of wave vector $\mathbf{k}$.
Θ - Photon perturbation.
Θ_l - l-th order multipole expansion term of Θ.
v_b - Baryon bulk velocity.
v_c - Cold dark matter bulk velocity.
v_γ - Photon bulk velocity.
δ_b - Baryon overdensity.
δ_c - Cold dark matter overdensity.
δ_γ - Photon overdensity.
ϕ - Inflaton field.
ρ_ϕ - Inflaton field density.
p_ϕ - Inflaton field pressure.
$\epsilon_{\text{sr}}, \delta_{\text{sr}}$ - Slow roll parameters.
$\mathcal{R}$ - Curvature perturbation.
$\mathcal{S}$ - Source function.

Density parameters

Density parameter $\Omega_X = \rho_X/\rho_c$ where ρ_X is the density and $\rho_c = 8\pi G/3H^2$ the critical density. X can take the following values:

b - Baryons.
CDM - Cold dark matter.
γ - Electromagnetic radiation.
ν - Neutrinos.
k - Spatial curvature.
Λ - Cosmological constant.

A 0 in the subscript indicates the present day value.

Fiducial cosmology

The fiducial cosmology used throughout this project is based on the observational data obtained by Aghanim et al. (2020):

$$
\begin{aligned}
h &= 0.67,\\
T_{\text{CMB0}} &= 2.7255\ \text{K},\\
N_{\text{eff}} &= 3.046,\\
\Omega_{\text{b0}} &= 0.05,\\
\Omega_{\text{CDM0}} &= 0.267,\\
\Omega_{k0} &= 0,\\
\Omega_{\nu 0} &= N_{\text{eff}} \cdot \frac{7}{8}\left(\frac{4}{11}\right)^{4/3} \Omega_{\gamma 0},\\
\Omega_{\Lambda 0} &= 1 - (\Omega_{k0} + \Omega_{\text{b0}} + \Omega_{\text{CDM0}} + \Omega_{\gamma 0} + \Omega_{\nu 0}),\\
\Omega_{\text{M0}} &= \Omega_{b0} + \Omega_{\text{CDM0}},\\
\Omega_{\text{rad}} &= \Omega_{\gamma 0} + \Omega_{\nu 0},\\
n_s &= 0.965,\\
A_s &= 2.1 \cdot 10^{-9}.
\end{aligned}
$$

Introduction

The Cosmic Microwave Background radiation is the leftover radiation from the early universe. It is the most ancient light we can observe, having travelled towards us ever since the Universe became transparent. Therefore, it contains a significant amount of information and it is of great interest to understand why it looks the way it does. Why are there fluctuations in the CMB? In this project we take a closer look at the CMB power spectrum. This is a plot that show the distribution of temperature fluctuations in the CMB across different angular scaler. This is of great significance to us, since the CMB power spectrum is able to reveal information about the cosmological parameters of our universe, such as the various density components and Hubble constant. It is also able to tell us something about the large scale structures of the Universe, and the overall geometry of space itself. Also, which is perhaps the most interesting, it can yield information about the nature of dark energy.

The overarching aim is to produce a pipeline that allows us to calculate numerically the CMB power spectrum given some cosmology. The steps will be presented chronologically, and we start by setting up the background cosmology in **??**. Here we solve the evolutionary equations for an isotropic and homogeneous universe using the ΛCDM-model. One particularly important event in the evolution of the CMB is recombination, ultimately leading to photon decoupling. After this, the photons free stream towards us and is what we today see as the CMB. The entire **??** is devoted to this event, and the time right before and right after it. In Section 1 we take a step away from the isotropic and homogeneous universe and consider perturbations to the metric in conformal Newtonian gauge. The implications these metric perturbations have on the distribution of matter is discussed, and we end up with a set of coupled differential equations that we can solve numerically. The initial condition of these are found by considering the period of inflation in the very early Universe.

TODO: Intro to Milestone 4

1. Perturbations

The aim of this section is to investigate how small fluctuations in the baryon-photon-dark-matter fluid in the early grew into larger structures. This is done by examining the interplay between these fluid fluctuations and the subsequent fluctuations of the space-time geometry. We will model this by perturbing the flat FLRW-metric using the conformal-Newtonian gauge. This will impact how the Boltzmann equations for the different species behaves, from which we are able to construct differential equations for key physical observables, and their initial conditions.

1.1. Theory

1.1.1. Metric perturbations

The perturbed metric in the conformal-Newtonian gauge is given in Callin (2006) as:

$$
g_{\mu\nu} = \begin{pmatrix} -(1+2\Psi) & 0 \\ 0 & e^{2x}\delta_{ij}(1+2\Phi) \end{pmatrix} \tag{1}
$$

This means that we perturb the FLRW-metric with $\Psi \ll 1$ corresponding to the Newtonian potential governing the motion of non-relativistic particles and $\Phi \ll 1$ governing the perturba-

tion of the spatial curvature. [1] The comoving momentum in this spacetime is:

$$P^\mu = \left[E(1-\Psi), p^i \frac{1-\Phi}{a}\right]. \tag{2}$$

By considering this momentum, and the geodesic equation in this perturbed spacetime we obtain the following (Dodelson & Schmidt 2020, Eqs. 3.62, 3.69, 3.71):

$$\frac{\mathrm{d}x^i}{\mathrm{d}t} = \frac{\hat{p}^i}{a}\frac{p}{E}(1-\Phi+\Psi) \tag{3a}$$

$$\frac{\mathrm{d}p^i}{\mathrm{d}t} = -\left(H + \frac{\mathrm{d}\Phi}{\mathrm{d}t}\right)p^i - \frac{E}{a}\frac{\partial\Phi}{\partial x^i} - \frac{1}{a}\frac{p^i}{E}p^k\frac{\partial\Phi}{\partial x^k} + \frac{p^2}{aE}\frac{\partial\Phi}{\partial x^i} \tag{3b}$$

$$\frac{\mathrm{d}p}{\mathrm{d}t} = -\left(H + \frac{\mathrm{d}\Phi}{\mathrm{d}t}\right)p - \frac{E}{a}\hat{p}^i\frac{\partial\Psi}{\partial x^i} \tag{3c}$$

Inserting Eq. (3) into **??**, and for now assuming $C[f] = 0$ yield the *collisionless Bolzmann equations*. Keeping terms to first order only,[2] yield the collisionless Bolzmann equation: (Dodelson & Schmidt 2020, Eq. 3.83):

$$\frac{\mathrm{d}f}{\mathrm{d}t} = \frac{\partial f}{\partial t} + \frac{p}{E}\frac{\hat{p}^i}{a}\frac{\partial f}{\partial x^i} - \left[H + \frac{\mathrm{d}\Phi}{\mathrm{d}t} + \frac{E}{ap}\hat{p}^i\frac{\partial\Psi}{\partial x^i}\right]p\frac{\partial f}{\partial p}. \tag{4}$$

Future work consists mainly of evaluating the collision terms for each species and equate it to Eq. (4)

1.1.2. Fourier space and multipole expansion

Consider a function $f(\mathbf{x}, t)$. Its Fourier transform $\mathscr{F}$ and inverse $\mathscr{F}^{-1}$ are defined as:

$$\mathscr{F}[f(\mathbf{x},t)] \equiv \frac{1}{(2\pi)^{3/2}}\int e^{-i\mathbf{k}\cdot\mathbf{x}} f(\mathbf{x},t)\mathrm{d}^3x = \tilde{f}(\mathbf{k},t), \tag{5}$$

$$\mathscr{F}^{-1}[\tilde{f}(\mathbf{k},t)] \equiv \frac{1}{(2\pi)^{3/2}}\int e^{i\mathbf{k}\cdot\mathbf{x}} \tilde{f}(\mathbf{k},t)\mathrm{d}^3k = f(\mathbf{x},t). \tag{6}$$

It becomes apparent from these definitions that taking the spatial derivative with respect to $\mathbf{x}$ in real space, is the same as multiplying the function with $i\mathbf{k}$ in Fourier space. This leads to the following property: $\mathscr{F}[\nabla f(\mathbf{x},t)] = i\mathbf{k}.\mathscr{F}[f(\mathbf{x},t)]$. This is of major significance when working with partial differential equations (PDEs), where:

$$\mathscr{F}[\nabla^2 f(\mathbf{x},t)] = i^2\mathbf{k}\cdot\mathbf{k}.\mathscr{F}[f(\mathbf{x},t)] = -k^2\mathscr{F}[f(\mathbf{x},t)]$$
$$\mathscr{F}\left[\frac{\mathrm{d}^n f(\mathbf{x},t)}{\mathrm{d}t^n}\right] = \frac{\mathrm{d}^n}{\mathrm{d}t^n}\mathscr{F}[f(\mathbf{x},t)]. \tag{7}$$

The two equations in Eq. (7) have the ability of reducing PDEs down to a set of decoupled ODEs. This means that we are able to solve for each mode $k = |\mathbf{k}|$ independently, which will be of great impact for the equations to come.

We will also work with multipole expansions, which are series written as sums of *Legendre polynomials* expanded in $\mu = \cos\theta \in [-1, 1]$ as:

$$f(\mu) = \sum_{l=0}^{\infty}\frac{2l+1}{i^l}f_l\mathcal{P}_l(\mu), \tag{8}$$

where $\mathcal{P}_l$ is the l-th Legendre polynomial. These are orthogonal in such a way that they form a complete basis, enabling us to express any $f(\mu)$ as in Eq. (8). The coefficients f_l are the *Legendre multipoles*:

$$f_l = \frac{i^l}{2}\int_{-1}^{1} f(\mu)\mathcal{P}_l(\mu)\mathrm{d}\mu. \tag{9}$$

The factors $(2l+1)/i^l$ in Eq. (8) and $i^l/2$ in Eq. (9) are just conventional choices. It is convenient to expand functions in this way when we are considering quantities that are function of a direction in the sky - since the Legendre polynomials are closely related to the spherical harmonics, which is a natural choice of basis for such quantities.

1.1.3. Einstein-Boltzmann equations

We have two perturbations to the metric, $\Phi(\mathbf{x}, t)$ to the spatial curvature, and $\Psi(\mathbf{x}, t)$ to the Newtonian potential. We seek to find the effect of these perturbations on baryonic matter, dark energy and radiation, as they "live" in a now perturbed spacetime. Let's start by defining the perturbation to the photons, $\Theta(\mathbf{x}, \hat{\mathbf{p}}, t)$, to be the variation of photon temperature around an equilibrium temperature $T^{(0)}$:

$$T(\mathbf{x},\hat{\mathbf{p}},t) = T^{(0)}\left[1 + \Theta(\mathbf{x},\hat{\mathbf{p}},t)\right]. \tag{10}$$

This is dependent on the location $\mathbf{x}$ and the direction of propagation $\hat{\mathbf{p}}$, thus capturing both inhomogeneities and anisotropies. We assume Θ to be independent of the momentum magnitude.[3] The collision terms for the photons are governed by Compton scattering. We use the form found in (Dodelson & Schmidt 2020, Eq. 5.22)TODO: assumptions: ignore polarisation, and angular dep. of thomson cross sec:

$$C[f(\mathbf{p})] = -p^2\frac{\partial f^{(0)}}{\partial p}n_e\sigma_T[\Theta_0 - \Theta(\hat{\mathbf{p}}) + \hat{\mathbf{p}}\cdot\mathbf{v}_b] \tag{11}$$

where Θ_0 is the monopole term.[4] $\mathbf{v}_b$ is the bulk velocity of the electrons involved in the process, and is the same as for baryons, hence the subscript. The distribution function for radiation follows the Bose-Einstein distribution function, so we expand f around its zeroth order Bose-Einstein form, (Dodelson & Schmidt 2020, Eq. 5.2-5.9), using the temperature perturbation in Eq. (10)TODO: Include equation 5.9 in Dodelson?. This is then inserted into Eq. (4), which we equate to the collision term in Eq. (11) in order to obtain the following full Boltzmann equation for radiation:[5]

$$\frac{\mathrm{d}\Theta}{\mathrm{d}t} + \frac{\hat{p}^i}{a}\frac{\partial\Theta}{\partial x^i} + \frac{\mathrm{d}\Phi}{\mathrm{d}t} + \frac{\hat{p}^i}{a}\frac{\partial\Psi}{\partial x^i} = n_e\sigma_T\left[\Theta_0 - \Theta + \hat{\mathbf{p}}\cdot\mathbf{v}_b\right] \tag{12}$$

For massive particles, we start with cold dark matter (CDM). Firstly, we assume cold dark matter to not interact with any other species, nor self-interact. Thus, we do not have any collision

[1] Φ may also be interpreted as a *local perturbation to the scale factor*, Dodelson & Schmidt (2020).

[2] This is justified by the ansatz that deviations away from the equilibrium distribution of radiation in the inhomogeneous universe are of same order as the spacetime perturbations Φ and Ψ, Dodelson & Schmidt (2020).

[3] This follows from the fact that the magnitude of the photon momentum is virtually unchanged by the dominant form of interaction, Compton scattering Dodelson & Schmidt (2020).

[4] This is the integral over the photon perturbation at any given point, over all photon directions. It is given by

$$\Theta_0(\mathbf{x},t) \equiv \frac{1}{4\pi}\int \mathrm{d}\Omega'\Theta(\mathbf{x},\hat{\mathbf{p}}',t)$$

where Ω' is the solid angle spanned by $\hat{\mathbf{p}}'$ Dodelson & Schmidt (2020).

[5] Where of course $m = 0 \iff E = p$.

terms. Further, we also assume it to behave like a fluid, neglecting any terms not to first order. We consider cold dark matter to be non-relativistic, thus they will only have a sizeable monopole and dipole term, which means that the evolution is fully characterised by the density and velocity, Winther et al. (2023). TODO: how much about moments should I explain? Therefore, we take the first and second moment of Eq. (4) and consider them to first order, in order to retrieve the cosmological generalisation of the continuity equation (Dodelson & Schmidt 2020, Eq. 5.41):

$$\frac{\partial n_c}{\partial t} + \frac{1}{a}\frac{\partial (n_c v_c^i)}{\partial x^i} + 3\left[H + \frac{\partial \Phi}{\partial t}\right] n_c = 0, \tag{13}$$

and the Euler equation (Dodelson & Schmidt 2020, Eq. 5.50):

$$\frac{\partial v_c^i}{\partial t} + H v_c^i + \frac{1}{a}\frac{\partial \Psi}{\partial x^i} = 0. \tag{14}$$

In both Eq. (13) and Eq. (14), n_c is the cold dark matter number density, $\mathbf{v}_c$ its bulk velocity. We then consider the perturbation of n_c to first order:

$$n_c(\mathbf{x}, t) = n_c^{(0)}[1 + \delta_c(\mathbf{x}, t)], \tag{15}$$

and consider the first order perturbation to Eq. (13):

$$\frac{\partial \delta_c}{\partial t} + \frac{1}{a}\frac{\partial v_c^i}{\partial x^i} + 3\frac{\partial \Phi}{\partial t} = 0. \tag{16}$$

Eq. (16) and Eq. (14) now described the evolution of the density perturbation δ_c and bulk velocity $\mathbf{v}_c$ of cold dark matter.

For baryons (protons and electrons) we also assume them to behave like a non-relativistic fluid, so taking moments is a similar task as for cold dark matter. The only difference is that baryons interact with each other through Coulomb scattering and Compton scattering. We may ignore Compton scattering between protons and photons due to the small cross-section, but electrons are coupled to both photons and protons. Since the first moment of the Boltzmann equation represents conservations of particle number, and none of the above interactions changes the total baryon particle number, the continuity equation is identical to Eq. (13), but for baryons. We also have a baryon perturbation similar to Eq. (15), which altogether results in the following density perturbation for baryons:

$$\frac{\partial \delta_b}{\partial t} + \frac{1}{a}\frac{\partial v_b^i}{\partial x^i} + 3\frac{\partial \Phi}{\partial t} = 0. \tag{17}$$

For the Euler equation, we now have to consider the collision terms, where momentum is conserved, but transferred between the baryons and photons. This collision term is found from considering the first moment of the photon distribution and find the momentum transfer due to Compton scattering. According to Winther et al. (2023) the momentum transfer in the baryon equation is $-n_e \sigma_T R^{-1}(v_\gamma^i - v_b^i)$, where R is defined in **??**. The Euler equation for baryons, similar to Eq. (14), but with the momentum transfer as source term now yield:

$$\frac{\partial v_b^i}{\partial t} + H v_b^i + \frac{1}{a}\frac{\partial \Psi}{\partial x^i} = -n_e \sigma_T R^{-1}(v_\gamma^i - v_b^i) \tag{18}$$

We have now acquired differential equations for the temperature fluctuations, Θ in Eq. (12), and the overdensities[6], δ_c, δ_b, and bulk velocities v_c^i and v_b^i, of cold dark matter and baryons respectively in Eq. (16), Eq. (17), Eq. (14) and Eq. (18). In order to make these differential equations easier to solve we make the transformation into Fourier space. We do this by introducing μ as the cosine of the angle between the Fourier wave vector $\mathbf{k}$ and the direction of the photon $\mathbf{p}/|\mathbf{p}|$. Additionally, velocities are generally longitudinal which enables us to write:

$$\mu \equiv \frac{\mathbf{k}\cdot\mathbf{p}}{kp}$$
$$\mathbf{v} = i\hat{\mathbf{k}} v \tag{19}$$

This enables us to summarise the differential equations as follows, now in Fourier space, and the time derivative is with respect to conformal time η:

$$\dot{\Theta} = -ik\mu(\Theta + \Psi) - \dot{\Phi} - \dot{\tau}\left[\Theta_0 - \Theta + i\mu v_b - \frac{\mathcal{P}_2\Theta_2}{2}\right], \tag{20a}$$
$$\dot{\delta}_c = -3\dot{\Phi} + k v_c, \tag{20b}$$
$$\dot{v}_c = -k\Psi - \mathcal{H} v_c, \tag{20c}$$
$$\dot{\delta}_b = -3\dot{\Phi} + k v_b, \tag{20d}$$
$$\dot{v}_b = -k\Psi + \dot{\tau} R^{-1}(v_b + 3\Theta_1) - \mathcal{H} v_b. \tag{20e}$$

In Eq. (20a) and Eq. (20e) we define $\dot{\tau}$ from **??**. Additionally, in Eq. (20a) we have included the term $\mathcal{P}_2\Theta_2/2$ in order to account for the angular dependency of Compton scattering previously ignored. We have also used that the photon velocity is proportional to the dipole $\Theta_1 = -v_\gamma/3$.

Our next step is to once again consider the perturbation to the metric in order to find out how the potentials Ψ and Φ change with time. In short, this is done by computing the perturbed Christoffel symbols using Eq. (1), finding the Ricci tensor and Ricci scalar, and construct the perturbed Einstein tensor. We also have to find the perturbed energy-momentum Tensor, and then solve the Einstein equation in **??**. The result yields the time evolution of Φ and Ψ, where we have from (Dodelson & Schmidt 2020, Eq. 6.41):

$$k^2\Phi + 3\mathcal{H}(\dot{\Phi} - \mathcal{H}\Psi) = 4\pi G a^2(\rho_c\delta_c + \rho_b\delta_b + 4\rho_\gamma\Theta_0), \tag{21}$$

and from (Dodelson & Schmidt 2020, Eq. 6.47)

$$k^2(\Phi + \Psi) = -32\pi G a^2(\rho_\gamma\Theta_2) : \tag{22}$$

Eq. (21) and Eq. (22) are both written in Fourier space. The final step is to write the photon fluctuations Θ as a hierarchy of multipoles in accordance with Eq. (8). The resultant hierarchy, along with all relevant equations, now written in terms of our preferred temporal variable x is given below:

[6] The fluctuations to the equilibrium densities.

Photon temperature multipoles

$$\Theta_0' = -\frac{ck}{\mathcal{H}}\Theta_1 - \Phi', \tag{23a}$$

$$\Theta_1' = \frac{ck}{3\mathcal{H}}\Theta_0 - \frac{2ck}{3\mathcal{H}}\Theta_2 + \frac{ck}{3\mathcal{H}}\Psi + \tau'\left[\Theta_1 + \frac{1}{3}v_b\right], \tag{23b}$$

$$\Theta_l' = \begin{cases} \frac{lck\Theta_{l-1}}{(2l+1)\mathcal{H}} - \frac{(l+1)ck\Theta_{l+1}}{(2l+1)\mathcal{H}} + \tau'\left[\Theta_l - \frac{\Theta_2}{10}\delta_{l,2}\right], & l \geq 2 \\ \frac{ck\Theta_{l-1}}{\mathcal{H}} - c\frac{(l+1)\Theta_l}{\mathcal{H}\eta} + \tau'\Theta_l, & l = l_\mathrm{f} \end{cases} \tag{23c}$$

Cold dark matter and baryons

$$\delta_c' = \frac{ck}{\mathcal{H}}v_c - 3\Phi', \tag{24a}$$

$$v_c' = -v_c - \frac{ck}{\mathcal{H}}\Psi, \tag{24b}$$

$$\delta_b' = \frac{ck}{\mathcal{H}}v_b - 3\Phi', \tag{24c}$$

$$v_b' = -v_b - \frac{ck}{\mathcal{H}}\Psi + \tau' R^{-1}(3\Theta_1 + v_b) \tag{24d}$$

Metric perturbations

$$\Phi' = \Psi - \frac{c^2k^2}{3\mathcal{H}^2}\Phi + \frac{\mathcal{Y}}{2}, \tag{25a}$$

$$\Psi = -\Phi - \frac{12\mathcal{H}^2}{c^2k^2}\Omega_\gamma\Theta_2. \tag{25b}$$

where $\mathcal{Y} = \Omega_c\delta_c + \Omega_b\delta_b + 4\Omega_\gamma\Theta_0$

1.1.4. Tight coupling regime

The tight coupling regime represents the time in the early Universe, before recombination, when both radiation, dark matter and baryons were tightly coupled together, interactions where frequent and efficient, and the primordial plasma very optically thick ($\tau \gg 1$). Due to this, the bulk velocity of the baryons (which co-moves with the other species due to the tight coupling) is very low. Furthermore, due to the frequent interactions and low bulk velocity the radiation dipole is suppressed. Altogether, this causes the combination $(3\Theta_1 + v_b)$ to be very small. The optical depth changes rapidly in the tight coupling regime, as seen from **??**, $|\tau'| \gg 1$. As a result, any combinations of the form $\tau'(\Theta_1 + v_b)$, as they occur in Eq. (23b) and Eq. (24d) are extremely numerically unstable. We therefore use said equations in order to rewrite for:

$$q = \frac{ck}{\mathcal{H}}(\Theta_0 - 2\Theta_2) + \tau'(1 + R^{-1})(3\Theta_1 + v_b) - v_b, \tag{26}$$

where we have defined

$$q \equiv (3\Theta_1 + v_b)' \implies \Theta_1' = (q - v_b')/3 \tag{27}$$

We are able to differentiate Eq. (26) w.r.t. x by using $(R^{-1})' = -R^{-1}$ in order to obtain:

$$\begin{aligned} q' = &\left[\tau''\left(1 + R^{-1}\right) + \left(1 - R^{-1}\right)\tau'\right](3\Theta_1 + v_b) \\ &+ \left[\tau'\left(1 + R^{-1}\right) - 1\right]q \\ &+ \frac{ck}{\mathcal{H}}\left(\Theta_0 - 2\Theta_2 + \Psi + \Theta_0' - 2\Theta_2' - \frac{\mathcal{H}'}{\mathcal{H}}(\Theta_0 - 2\Theta_2)\right) \end{aligned} \tag{28}$$

The treatment leading up to Eq. (28) is exact, but now we make the following approximation, Winther et al. (2023): In a radiation dominated universe (which is what we have in the tight coupling regime) we have that:

$$\begin{aligned} \eta \propto a \propto \tau'^{-1} \propto (3\Theta_1 + v_b) &\implies \frac{\mathrm{d}^2}{\mathrm{d}\eta^2}(3\Theta_1 + v_b) \approx 0 \\ &\implies q' \approx -\frac{\mathcal{H}'}{\mathcal{H}}q \end{aligned} \tag{29}$$

We find q by equating Eq. (28) and Eq. (29) and solving for q. We further use Eq. (26) and solve for $\tau'(1 + R^{-1})(3\Theta_1 + v_b)$ which we substitute into Eq. (24d) in order to obtain an equation for v_b'. Altogether, this give rise to the following equations, valid in the tight coupling regime:

Tight coupling equations

$$\begin{aligned} q\left[(1 + R^{-1})\tau' + \frac{\mathcal{H}'}{\mathcal{H}} - 1\right] = &\\ -\left[\tau''\left(1 + R^{-1}\right) + \left(1 - R^{-1}\right)\tau'\right](3\Theta_1 + v_b) &\\ -\frac{ck}{\mathcal{H}}\Psi + \left(1 - \frac{\mathcal{H}'}{\mathcal{H}}\right)\frac{ck}{\mathcal{H}}(-\Theta_0 + 2\Theta_2) - \frac{ck}{\mathcal{H}}\Theta_0' & \end{aligned} \tag{30}$$

$$\begin{aligned} v_b'\left[1 + R^{-1}\right] = &-v_b - \frac{ck}{\mathcal{H}}\Psi \\ &+ R^{-1}\left(q + \frac{ck}{\mathcal{H}}(-\Theta_0 + 2\Theta_2) - \frac{ck}{\mathcal{H}}\Psi\right) \end{aligned} \tag{31}$$

$$\Theta_1' = \frac{1}{3}(q - v_b'), \tag{32a}$$

$$\Theta_2 = -\frac{20ck}{45\mathcal{H}\tau'}\Theta_1, \tag{32b}$$

$$\Theta_l = -\frac{l}{2l+1}\frac{ck}{\mathcal{H}\tau'}\Theta_{l-1} \quad l > 2. \tag{32c}$$

1.1.5. Modes, scales and the horizon

It is now useful to stop and ponder about what we have achieved so far. We have derived a set of differential equations for the perturbation of cosmological observables. Physically, these perturbations are spatial, but during the derivation we transformed all the equations into Fourier space, whose virtue is to remove the spatial dependency. Instead, the equations are expressed in terms of the *Fourier mode* k. Each *k-mode* is characterised by a comoving wavenumber $\mathbf{k}$, whose angular dependency is contained in the multipole expansion. Thus, we are left with the scalar k to represent the original spatial distribution, and indeed; each k represent a unique *spatial scale*. This is because the Fourier transform decompose the spatial function into its frequency components, and each k represent a certain frequency, inverse proportional to the wavelength, which represent the physical spatial scale.

Thus, small k-modes represents large wavelengths which in this context mean perturbations on large scales. On the other hand, large k-modes represents small-scale perturbations. What

is large and what is small is typically defined through the conformal horizon η, as represented in figure **??**, which is a measure of the causally connected regions of the Universe. We follow the definitions of the different regimes as given in Dodelson & Schmidt (2020):

$$\begin{aligned} k\eta &\ll 1 \quad \text{large scale modes,} \\ k\eta &\simeq 1 \quad \text{intermediate scale modes,} \\ k\eta &\gg 1 \quad \text{small scale modes.} \end{aligned} \tag{33}$$

The horizon will evolve in time, and we thus expect these modes at different scales to also evolve differently in time. At very early times, the horizon is very small, and we expect add modes to be larger than this. We thus define the concept of *super-horizon* modes, which are modes whose scale is larger than the horizon. We ultimately also have *sub-horzon* modes, where the scale is smaller than the horizon. Different modes are expected to undergo *horizon crossing* at different times.

As a result of this Fourier decomposition, we can investigate what happens at different scales for the various perturbations. In order to re-express the perturbations as function of a physical quantity, say $\mathbf{x}$,[7] we need to integrate across all the different k-modes, basically accumulating the contributions to the perturbation across all scales.

1.1.6. Inflation

To be able to numerically integrate Eq. (23), Eq. (24) and Eq. (25) we must determine the initial conditions of each quantity. Thus, we need to know how the Universe behaved at a very early stage. It is proposed that an epoch called *inflation* took place, during which the Universe exponentially increases in size during a very short period of time Dodelson & Schmidt (2020).[8] We will describe the inflationary period in order to obtain the initial conditions of the metric perturbations Ψ and Φ.

Assume inflation is driven by a scalar field $\phi(t, \mathbf{x})$, typically referred to as *inflaton field*. For inflation to happen, the acceleration of the scale factor must be positive, meaning that the inflaton field must model a fluid where the equation of state parameter ω is negative, i.e. $3p+\rho < 0$. By considering the temporal and spatial part of the energy-momentum tensor, Dodelson & Schmidt (2020) obtains the following equations for the pressure and density of the inflaton field:

$$\rho_\phi = \frac{1}{2}\left(\frac{\mathrm{d}\phi}{\mathrm{d}t}\right)^2 + V(\phi), \tag{34}$$

and

$$p_\phi = \frac{1}{2}\left(\frac{\mathrm{d}\phi}{\mathrm{d}t}\right)^2 - V(\phi), \tag{35}$$

where $1/2\left(\frac{\mathrm{d}\phi}{\mathrm{d}t}\right)^2$ is the kinetic energy of the field, and $V(\phi)$ is the potential energy. Thus, $\omega = p/\rho < 0$ implies that the inflaton field must have more potential than kinetic energy. We therefore require it to *roll slowly* in the potential, and thus introduce the *slow roll parameters* ϵ_{sr} and δ_{sr}, both of which must be satisfied for the field to be able to perform inflation. These are:

$$\epsilon_{\mathrm{sr}} = \frac{E_{\mathrm{pl}}^2}{16\pi}\left(\frac{V'}{V}\right)^2 \ll 1 \tag{36a}$$

$$\delta_{\mathrm{sr}} = \frac{E_{\mathrm{pl}}}{8\pi}\left(\frac{V''}{V}\right) \ll 1, \tag{36b}$$

where the derivative of the potential V is in terms of ϕ.

Next, one of the crucial assumptions is that we can express the inflaton field in terms of a perturbation (or overdensity) as:

$$\phi(t, \mathbf{x}) = \phi^{(0)}(t) + \delta\phi(t, \mathbf{x}), \tag{37}$$

where $\phi^{(0)}$ is the equilibrium value of the field, only dependent on time. We will concern ourselves with the perturbation $\delta\phi$ and investigate what happens to it during the inflationary period. Before inflation, we expect $\Psi = \Phi = 0$ and the perturbation $\delta\phi$ to be of quantum nature.

TODO: fill more here maybe

We could in principle solve the full Einstein equation where Ψ and Φ enters through the Einstein tensor, and ϕ through the energy-momentum tensor.[9] This is not trivial, and instead we introduce the curvature perturbation $\mathcal{R}(\delta\phi, \Psi)$, which is a conserved quantity, as Dodelson & Schmidt (2020):

$$\mathcal{R} = -\frac{ik_i\delta T_i^0}{k^2(p+\rho)} - \Psi, \tag{38}$$

where k is the mode (in Fourier space), $T_0^i = g^{iv} = \partial_\nu\phi\partial_0\phi$ is the spatial part of the energy-momentum tensor, and p and ρ are the pressure and density.

If we consider the situation before inflation, assume $\Psi = 0$. From Eq. (36) we have that $\rho + p = \dot{\phi}^2/a^2$ using conformal time. Further, according to (Dodelson & Schmidt 2020, Eq. 7.47), $\delta T_0^i = ik_i\dot{\phi}\delta\phi/a^3$. Inserting this into Eq. (38) yield before inflation:

$$\mathcal{R}_{\mathrm{initial}} = -aH\frac{\delta\phi}{\dot{\phi}}. \tag{39}$$

Looking at the same situation at the end of inflation, we now assume radiation domination: $p = \rho/3$. According to Dodelson & Schmidt (2020), $ik_i\delta T_0^i = -4k\rho_\gamma\Theta_1/a$ in the radiation dominated era. Inserting this into Eq. (38) yield:

$$\mathcal{R}_{\mathrm{end}} = -\frac{3aH\Theta_1}{k} - \Psi = -\frac{3}{2}\Psi, \tag{40}$$

where the last equality comes from the postulate that the initial condition for the dipole is $\Theta_1 = -k\Phi/6aH$, which will we showed in the following section. For the sake of completeness, we not equate Eq. (39) and Eq. (40) to obtain:

$$\Psi = \frac{2}{3}aH\frac{\delta\phi}{\dot{\phi}}\Big|_{\text{horizon crossing}}, \tag{41}$$

which is the value of Ψ immediately after inflation, when the mode is of equal size as the horizon (hence horizon crossing). TODO: check if this actually is correct

[7] This is the physical spatial variable, $\mathbf{x}$, representing a position. If you thought this was a vector quantity of the temporal quantity $x = \ln a$ you need to evaluate your choices in life.

[8] An inflationary process would also solve the horizon problem, the flatness problem and the monopole problem amongst other things. Details about this can be found in both Dodelson & Schmidt (2020), Carroll (2019), and Weinberg (2008).

[9] The energy-momentum tensor for ϕ is given in (Dodelson & Schmidt 2020, Eq. 7.6) as:

$$T^\alpha{}_\beta = g^{\alpha\nu}\frac{\partial\phi}{\partial x^\nu}\frac{\partial\phi}{\partial x^\beta} - \delta^\alpha{}_\beta\left[\frac{1}{2}g^{\mu\nu}\frac{\partial\phi}{\partial x^\mu}\frac{\partial\phi}{\partial x^\nu} + V(\phi)\right].$$

1.1.7. Initial conditions

We now seek to determine the actual initial conditions enabling us to solve the desired differential equations. At very early times, we make the following assumptions:

$$k\eta \ll 1 \iff \frac{k}{\mathcal{H}} \ll 1 \tag{42a}$$
$$\tau \gg 1 \text{ and } \left|\tau'\right| \gg 1 \tag{42b}$$
$$\Theta_0 \gg \Theta_1 \gg \Theta_2 \gg \cdots \gg \Theta_l. \tag{42c}$$

Eq. (42a) is necessary in order to ensure causally disconnected regions in the early universe. It also ensures that the modes we are interested in today is outside the horizon Winther et al. (2023). We have already established that the universe is optically thick, so Eq. (42b) follow directly from **??**. Further, at these scales we expect the lower multipoles to be dominant, thus Eq. (42c) holds. This is because the causal horizon is smaller than the k-modes, making the radiation observed by an hypothetical observer nearly uniform. Applying the assumptions in Eq. (42) to Eq. (23), Eq. (24) and Eq. (25) allows to determine the initial conditions.

Firstly, the perturbations of Φ and Ψ evolves slowly outside the horizon, so we may approximate $\Phi' = \Psi' = 0$. However, we will use their expression in order to determine other initial conditions. In the following we make use of the assumptions in Eq. (42). Eq. (23a) becomes $\Theta_0' = -\Phi'$. Further, Eq. (25a) turn into $\Phi' = \Psi + 2\Theta_0 \implies \Theta_0 = -\Psi/2$. The overdensities Eq. (24c) and Eq. (24a) have similar behaviour[10] and we write $\delta' = -3\Phi' = 3\Theta_0'$. Integrating both sides yield $\delta = -3\Psi/2 + C$, where C is the integration constant. This is put to zero, making the initial conditions *adiabatic*. Eq. (25b) now fixes the relation between the initial conditions of Ψ and Φ as $\Phi = -\Psi$.

For the velocities, we expect the baryon and cold dark matter velocities to have the same initial value, and we find it by considering Eq. (24b), which can be written as $(va)' = -cka\Psi/\mathcal{H}$. Integration yields $v = -ck\Psi/2\mathcal{H}$ where we have omitted the constant of integration. We find the initial conditions for the next multipole terms by following a similar logic. This is also shown in (Dodelson & Schmidt 2020, Eq. 7.59) which fixes the velocities as $v = 3ck\Phi/6\mathcal{H}$,[11] and gives the initial dipole moment $\Theta_1 = -k\Phi/6aH$. Inserting this into Eq. (40) yields the desired $\mathcal{R} = -2\Psi/2$. Since $\mathcal{R}$ is conserved, choosing a value for it equations to fixing a normalisation. We will simply use $\mathcal{R} = 1$. The full set of adiabatic initial conditions then become:

Initial conditions

$$\Psi = -\frac{2}{3}, \tag{43a}$$
$$\Phi = -\Psi, \tag{43b}$$
$$\delta_c = \delta_b = -\frac{3}{2}\Psi, \tag{43c}$$
$$v_c = v_b = -\frac{ck}{2\mathcal{H}}\Psi, \tag{43d}$$
$$\Theta_0 = -\frac{1}{2}\Psi, \tag{43e}$$
$$\Theta_1 = \frac{ck}{6\mathcal{H}}\Psi, \tag{43f}$$
$$\Theta_2 = -\frac{20ck}{45\mathcal{H}\tau'}\Theta_1, \tag{43g}$$
$$\Theta_l = -\frac{l}{2l+1}\frac{ck}{\mathcal{H}\tau'}\Theta_{l-1}. \tag{43h}$$

1.1.8. Line of sight integration

TODO: Sow discussion together, why is this important, iterative scheme etc. The idea behind the line of sight integration was first proposed by Seljak & Zaldarriaga (1996), where instead of expanding the photon perturbation in multipoles and then integrating, the integral is solved explicitly and expanded into multipoles at the end. The gist of the derivation is to start with Eq. (20a) and rewrite it into a form: $\dot{\Theta} + (ik\eta - \dot{\tau}) = S$, where S is for now just a source term. [12] This can be rewritten into:

$$e^{-ik\mu\eta+\tau}\frac{\mathrm{d}}{\mathrm{d}\eta}\left[\Theta e^{ik\mu\eta-\tau}\right] = S, \tag{44}$$

which we can integrate by parts to obtain:

$$\Theta(k,\mu,\eta_0) = \int_{\eta_i}^{\eta_0} S\, e^{ik\mu(\eta-\eta_0)-\tau}\mathrm{d}\eta, \tag{45}$$

where η_0 is the conformal time today and η_i is the initial time from which we start integrating. Eq. (45) tells us physically that in order to obtain the photon perturbation today, we can integrate an exponentially attenuated source term along the past light cone of the photon. [13] Then, following the discussion in (Dodelson & Schmidt 2020, Eq. 9.49 - Eq. 9.54) we are able to decompose Eq. (45) into its individual multipoles, now expressed in terms of x:

$$\Theta_l(k, x=0) = \int_{-\infty}^{0} \mathcal{S}(k,x)\, j_l\left[k(\eta_0 - \eta(x))\right]\mathrm{d}x, \tag{46}$$

where $j_l\left[k(\eta_0 - \eta(x))\right]$ are the spherical Bessel functions. $\mathcal{S}(k,x)$ is known as the *source function* and is given by:

$$\mathcal{S}(k,x) = \tilde{g}\left[\Theta_0 + \Psi + \frac{\Theta_2}{4}\right] + e^{-\tau}\left[\Psi' - \Phi'\right] - \frac{1}{ck}\frac{\mathrm{d}}{\mathrm{d}x}\left[\mathcal{H}\tilde{g}v_b\right] + \frac{3}{4c^2k^2}\frac{\mathrm{d}}{\mathrm{d}x}\left[\mathcal{H}\frac{\mathrm{d}}{\mathrm{d}x}\left(\mathcal{H}\tilde{g}\Theta_2\right)\right]. \tag{47}$$

Due to the nature of the product rule, Eq. (47) end up containing a lot of terms. We state the individual result of the differentiated

[10] Because gravity does not care whether it acts on baryons or dark matter.

[11] Dodelson & Schmidt (2020) uses iv as velocities, but we have multiplied the velocities with i in order to make them real, but ultimately changing signs.

[12] Will return to this later.

[13] Hence the name: line of sight integration.

terms below:

$$\frac{\mathrm{d}}{\mathrm{d}x}\left[\mathcal{H}\tilde{g}v_b\right] = \mathcal{H}\tilde{g}v_b' + \mathcal{H}\tilde{g}'v_b + \mathcal{H}'\tilde{g}v_b \tag{48}$$

and

$$\begin{aligned}\frac{\mathrm{d}}{\mathrm{d}x}\left[\mathcal{H}\frac{\mathrm{d}}{\mathrm{d}x}\left(\mathcal{H}\tilde{g}\Theta_2\right)\right] &= \tilde{g}\Theta_2\left[\mathcal{H}''\mathcal{H} + \left(\mathcal{H}'\right)^2\right] \\ &+ \mathcal{H}^2\left[\tilde{g}\Theta_2'' + \tilde{g}''\Theta_2 + 2\tilde{g}'\Theta_2'\right] \\ &+ 3\mathcal{H}'\mathcal{H}\left[\tilde{g}\Theta_2' + \tilde{g}'\Theta_2\right].\end{aligned} \tag{49}$$

In order to find Θ_2'' we insert $l = 2$ in Eq. (23c) and differentiate:

$$\begin{aligned}\Theta_2'' &= \frac{\mathrm{d}}{\mathrm{d}x}\left[\frac{2ck}{5\mathcal{H}}\Theta_1 - \frac{3ck}{5\mathcal{H}}\Theta_3 + \tau'\left(\Theta_2 - \frac{\Theta_2}{10}\right)\right] \\ &= \frac{2ck}{\mathcal{H}}\left(\Theta_1' - \frac{\mathcal{H}'}{\mathcal{H}}\Theta_1\right) + \frac{3ck}{5\mathcal{H}}\left(\frac{\mathcal{H}'}{\mathcal{H}}\Theta_3 - \Theta_3'\right) \\ &+ \frac{9}{10}\left(\tau''\Theta_2 + \tau'\Theta_2'\right)\end{aligned} \tag{50}$$

1.2. Methods

TODO: more here maybe It is now time to find solutions to the equations we have developed. The first task is to determine when we have to use the tight coupling equations in Eq. (30), Eq. (31) and Eq. (32). As discussed in Section 1.1.4, the tight coupling regime should be used for early times, when $\tau, |\tau'| \gg 1$. We expect it to last no longer than until recombination, and thus define a higher threshold of $x = -8.3$. We also have from Callin (2006) that $ck/(\mathcal{H}\tau') \ll 1$ during tight coupling. Therefore, we adopt the following conditions, all of which must be satisfied for the tight coupling regime to be valid:

$$\begin{aligned}\left|\frac{\mathrm{d}\tau}{\mathrm{d}x}\right| &= \tau' > 10 \\ \left|\frac{\mathrm{d}\tau}{\mathrm{d}x}\right| &= \tau' > \frac{10ck}{\mathcal{H}} \\ x &< -8.3\end{aligned} \tag{51}$$

As soon as one of the above conditions fails, we must adopt the full system described in Eq. (23), Eq. (24) and Eq. (25). It is therefore wise to implement a routine that finds $x = x_{\mathrm{tc}}$ which will be the transition between tight coupling and the full system. This value will change with k.

When integrating we use uniformly spaced values of $x \in [-20, 0]$ and logarithmically spaced values of $k \in [0.00005, 0.3]$/Mpc. This should The differential equations are then solved with the initial conditions from Eq. (43) for $x \in [-20, x_{\mathrm{tc}}]$. After tight coupling, the differential equations are solved with initial conditions given as the last solution of the tight coupling equations, for $x \in (x_{\mathrm{tc}}, 0]$. At the end, both solutions (for all k-s) are "sown" together using the same x-array, and splined for all x and k.

When finding the source function we use the same x and k arrays as in the section above, and solve Eq. (47) for each combination. The result is then splined.

When analysing the results, we choose k-modes from all the regimes described in Section 1.1.5: $k_1 = 0.001$/Mpc as the large scale mode, $k_2 = 0.01$/Mpc as the intermediate scale mode and $k_3 = 0.1$/Mpc as the small scale mode.

1.3. Results and discussion

1.3.1. Potentials

Fig. 1 shows the metric perturbation potentials Φ and Ψ as functions of time x for the k-modes under investigation. The time of matter-radiation equality and recombination is marked in the plot as black dash-dotted and dashed lines respectively. Let's first consider the top panel, showing only Φ. At early times, it seems to be constant across all k-modes. [14] This is expected since at early times, the horizon is small and most modes are larger than this. Thus, they will be unaffected by causal physics and stay constant at their initial value. As time proceeds, the smaller k-modes will be surpassed by the horizon and are suddenly subjected to causal physics. We see from the top panel that if this happens in the radiation dominated regime (before radiation-matter equality), the potential will decline as e^{-2x}. This can be seen from Eq. (25a). However, for large scale modes, like the blue graph, where horizon crossing happens in the matter dominated regimes, then we expect the potential to decline with a factor 9/10 as it transitions from radiation domination to matter domination.

The sum of the potentials in the bottom panel of Fig. 1 goes as $\Psi + \Phi \sim e^{-2x}/k^2\Theta_2$, so it will closely follow the quadrupole term, but being suppressed by an exponential factor. Also, the k^2 term suggested larger value for small k-s (large scale). We save the discussion of the quadrupole, but the latter can clearly be seen as the large and intermediate scale modes show sinusoidal behaviour, with the large scale mode having a larger amplitude. Both are exponentially suppressed. These effects happen when the tight coupling epoch is over, since all multipoles except the monopole and dipole are suppressed during tight coupling.

1.3.2. Multipoles

We now focus our attention on the multipoles, starting with the monopole term expressed through the photon overdensity $\delta_\gamma = 4\Theta_0$. Mathematically, this relation can be seen from either the parenthesis in Eq. (21) or the definition of $\mathcal{Y}$ in Eq. (25) following somewhat diffuse symmetry arguments. Physically it also makes sense since the photon monopole is some measure of the average photon temperature which intuitively can be though of as a photon overdensity. It can be seen for the various k-modes in Fig. 2, where we clearly see that the small scale perturbation undergoes horizon crossing first, and become subject to causal physics. This is manifest in the oscillation of the green curve in the figure. Metric perturbations and pressure will generate acoustic oscillations within causally connected regions. When the horizon increase, these oscillations will affect a spatially large area, affecting k-modes on larger and larger scales. This is also manifest in Fig. 2 as the intermediate k-mode starts to oscillate later, and finally the large scale mode.

A similar discussion to the one above can be applied on the photon velocity $v_\gamma = -3\Theta_1$, as shown in Fig. 3. Similarly to the monopole, small scale modes enter the horizon first and starts to oscillate followed by larger scale modes.

The same is the case for the quadrupole in Fig. 4. However, as previously assumed, the quadrupole term is strongly suppressed during tight coupling, but behave similarly to the lower order multipoles after tight coupling. Considering the large and intermediate scale modes (blue and red curve) we are able to

[14] When referring to "all k-modes" it is implicit that we only mean the three modes considered here, but the qualitative discussions should be valid across all k-modes.

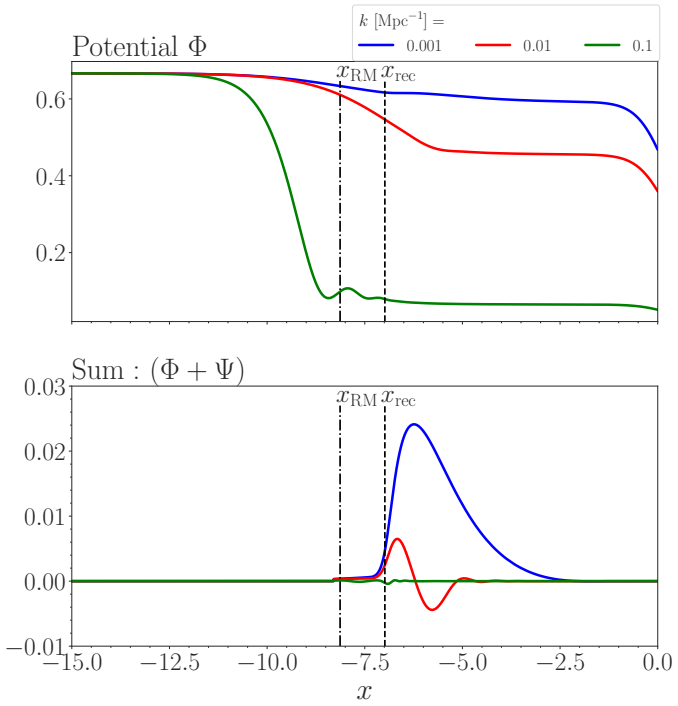

Fig. 1. The metric perturbation potentials, Ψ representing the Newtonian potential, and Φ representing the spatial curvature perturbations. Both panels show the evolution as function of the time x, for the three different k-modes outlined in Section 1.2. The top panel shows Φ alone, while the bottom shows the sum of the two. The dashed black line is the time of recombination as found in **??**, and the dash-dotted black line is the time of radiation-matter equality as found in **??**.

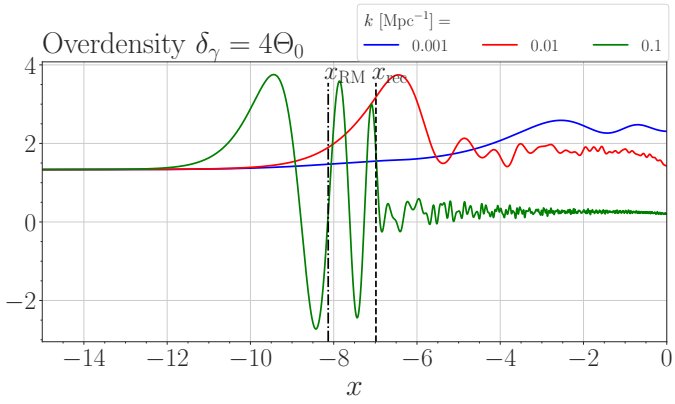

Fig. 2. Photon overdensity represented by the photon monopole for the various k-modes. The dashed black line is the time of recombination, and the dash-dotted black line is the time of radiation-matter equality.

close the discussion of the sum of potential in Fig. 1, where the quadrupole was the main contributor to the sinusoidal frequency, and k to the amplitude.

1.3.3. Matter perturbations

For the matter perturbations, we start with the overdensities for cold dark matter and baryons, shown in Fig. 5. Intuitively, we would expect small fluctuations in density to occur at very small scales early on, and then at larger scales gradually as the horizon increase. During the radiation dominated regime, expect the matter densities to be relatively homogenous on large scales, but noticeable on small scaler. In the matter dominated regime we expect overdense regions to attract more and more matter, increasing the overdensities. These effect should be noticeable on larger scales even, i.e. the modes that undergo horizon crossing during matter dominatin. When inspecting Fig. 5 this is indeed what we observe. The overdensity of the small scale mode in green starts to increase during radiation domination, large scale mode in blue during matter domination and the intermediate scale mode in red somewhere in between. All modes increase during matter domination which is what we expected. During dark energy domination we would expect the acceleration of the Universe to start to break up some structures and decrease the horizon, which would also decrease the matter overdensities. Lastly, we take note of the oscillations in the baryon density right before and after matter-radiation equality, but save the discussion for later.

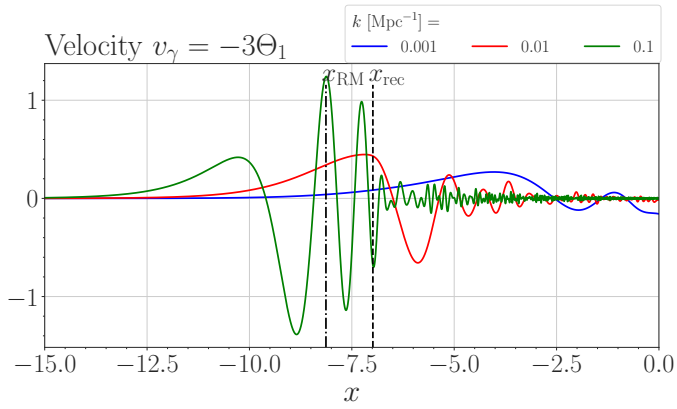

Fig. 3. Photon velocity represented by the photon dipole for the various k-mdoes. term The dashed black line is the time of recombination, and the dash-dotted black line is the time of radiation-matter equality.

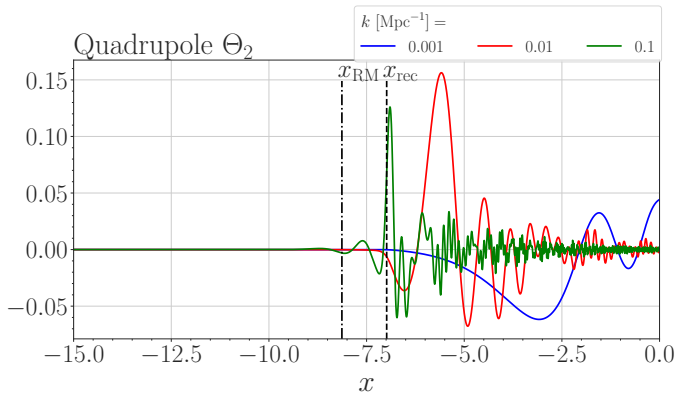

Fig. 4. Quadrapole term of the photon perturbation. This term only becomes relevant after tight coupling. The dashed black line is the time of recombination, and the dash-dotted black line is the time of radiation-matter equality.

The next thing to consider are the matter velocities, shown in Fig. 6 TODO: Comment these

The remaining question to answer now is why does the baryon overdensity and velocity oscillate for the modes entering the horizon during radiation domination? In order to answer this question we consider the largest mode among the three; $k = 0.1$/Mpc, and plot the velocities and overdensities of the cold dark matter, baryons and photons in the same plot. The result is seen in Fig. 7 for the velocities and in Fig. 8 for the overdensities. We have already made statements about the oscil-

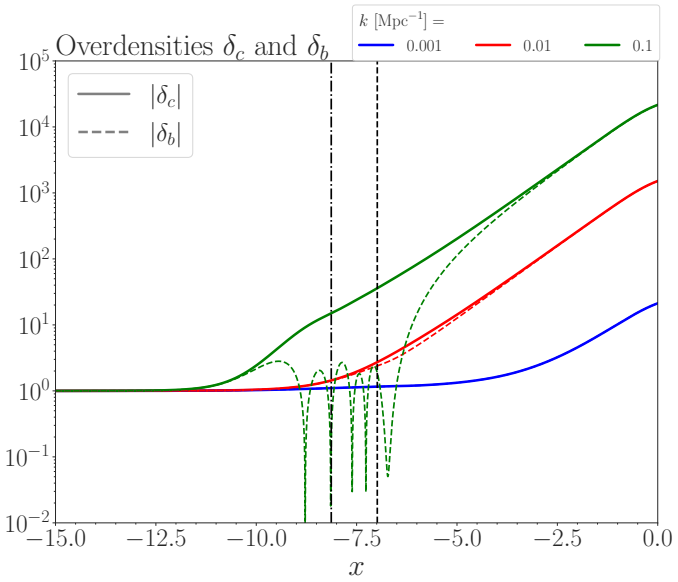

Fig. 5. The overdensities of cold dark matter and barons for the various k-modes. The dashed black line is the time of recombination, and the dash-dotted black line is the time of radiation-matter equality.

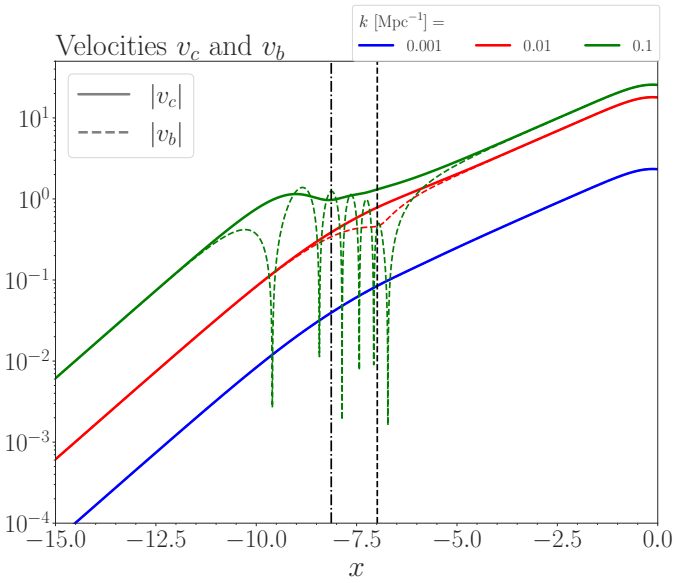

Fig. 6. Velocities term

lation of the photon velocity from Fig. 3, and photon overdensity from Fig. 2. The most important time in Fig. 7 and Fig. 8 is the time of recombination (dashed line), which is closely related to the time of decoupling and last scattering, when the photons decouple from the baryons. Before this, baryons and photons are tightly coupled so we expect them to evolve similarly. It therefore makes sense that we have oscillations in the baryon velocity and overdensity before recombinations, as the baryons were tightly coupled to the photons. After decoupling, the baryon velocity and overdensity show similar behaviour to those of cold dark matter. At the same time, the oscillations of the photon monopole and dipole causes the photon velocity and overdensity to gradually decrease and converge as the photons free stream through the Universe.

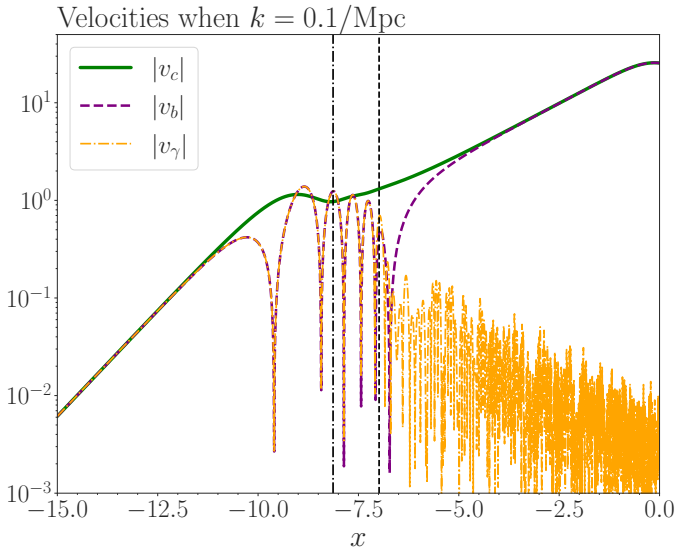

Fig. 7. Velocities term

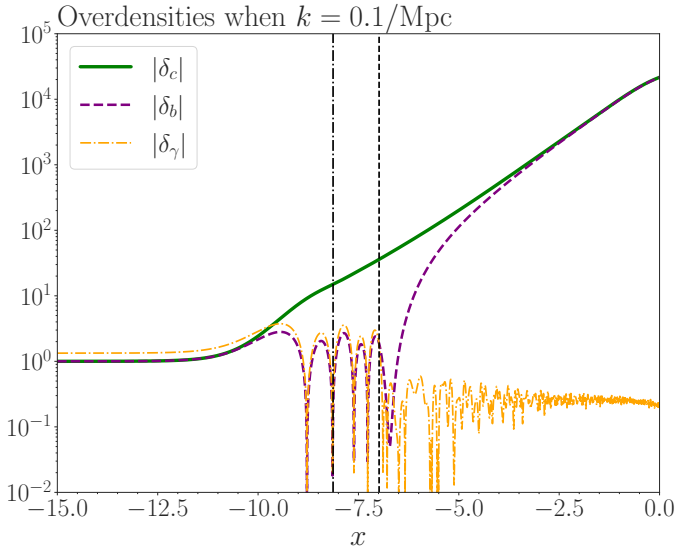

Fig. 8. Velocities term

References

Aghanim, N., Akrami, Y., Ashdown, M., et al. 2020, Astronomy & Astrophysics, 641, A6

Callin, P. 2006, How to calculate the CMB spectrum

Carroll, S. M. 2019, Spacetime and Geometry: An Introduction to General Relativity (Cambridge University Press)

Dodelson, S. & Schmidt, F. 2020, Modern Cosmology (Elsevier Science)

Seljak, U. & Zaldarriaga, M. 1996, The Astrophysical Journal, 469, 437

Weinberg, S. 2008, Cosmology, Cosmology (OUP Oxford)

Winther, H. A., Eriksen, H. K., Elgaroy, O., Mota, D. F., & Ihle, H. 2023, Cosmology II, https://cmb.wintherscoming.no/, accessed on March 1, 2023

Appendix A: Useful derivations

A.1. Angular diameter distance

This is related to the physical distance of say, an object, whose extent is small compared to the distance at which we observe is. If the extension of the object is Δs, and we measure an angular size of $\Delta\theta$, then the angular distance to the object is:

$$d_A = \frac{\Delta s}{\Delta\theta} = \frac{\mathrm{d}s}{\mathrm{d}\theta} = \sqrt{e^{2x}r^2} = e^x r, \tag{A.1}$$

where we inserted for the line element $\mathrm{d}s$ as given in equation **??**, and used the fact that $\mathrm{d}t/\mathrm{d}\theta = \mathrm{d}r/\mathrm{d}\theta = \mathrm{d}\phi/\mathrm{d}\theta = 0$ in polar coordinates.

A.2. Luminosity distance

If the intrinsic luminosity, L of an object is known, we can calculate the flux as: $F = L/(4\pi d_L^2)$, where d_L is the luminosity distance. It is a measure of how much the light has dimmed when travelling from the source to the observer. For further analysis we observe that the luminosity of objects moving away from us is changing by a factor a^{-4} due to the energy loss of electromagnetic radiation, and the observed flux is changed by a factor $1/(4\pi d_A^2)$. From this we draw the conclusion that the luminosity distance may be written as:

$$d_L = \sqrt{\frac{L}{4\pi F}} = \sqrt{\frac{d_A^2}{a^4}} = e^{-x} r \tag{A.2}$$

A.3. Differential equations

From the definition of $e^x \mathrm{d}\eta = c\mathrm{d}t$ we have the following:

$$\begin{aligned} &\frac{\mathrm{d}\eta}{\mathrm{d}t} = \frac{\mathrm{d}\eta}{\mathrm{d}x}\frac{\mathrm{d}x}{\mathrm{d}t} = \frac{\mathrm{d}\eta}{\mathrm{d}x}H = e^{-x}c \\ \implies &\frac{\mathrm{d}\eta}{\mathrm{d}x} = \frac{c}{\mathcal{H}}. \end{aligned} \tag{A.3}$$

Likewise, for t we have:

$$\begin{aligned} &\frac{\mathrm{d}\eta}{\mathrm{d}t} = \frac{\mathrm{d}\eta}{\mathrm{d}x}\frac{\mathrm{d}x}{\mathrm{d}t} = \frac{\mathrm{d}x}{\mathrm{d}t}\frac{c}{\mathcal{H}} = e^{-x}c \\ \implies &\frac{\mathrm{d}t}{\mathrm{d}x} = \frac{e^x}{\mathcal{H}} = \frac{1}{H}. \end{aligned} \tag{A.4}$$

Appendix B: Sanity checks

B.1. For $\mathcal{H}$

We start with the Hubble equation from **??** and realize that we may write any derivative of U as

$$\frac{\mathrm{d}^n U}{\mathrm{d}x^n} = \sum_i (-\alpha_i)^n \Omega_{i0} e^{-\alpha_i x}. \tag{B.1}$$

We further have:

$$\frac{\mathrm{d}\mathcal{H}}{\mathrm{d}x} = \frac{H_0}{2} U^{-\frac{1}{2}} \frac{\mathrm{d}U}{\mathrm{d}x}, \tag{B.2}$$

and

$$\begin{aligned} \frac{\mathrm{d}^2\mathcal{H}}{\mathrm{d}x^2} &= \frac{\mathrm{d}}{\mathrm{d}x}\frac{\mathrm{d}\mathcal{H}}{\mathrm{d}x} \\ &= \frac{H_0}{2}\left[\frac{\mathrm{d}U}{\mathrm{d}x}\left(\frac{\mathrm{d}}{\mathrm{d}x}U^{-\frac{1}{2}}\right) + U^{-\frac{1}{2}}\left(\frac{\mathrm{d}}{\mathrm{d}x}\frac{\mathrm{d}U}{\mathrm{d}x}\right)\right] \\ &= H_0\left[\frac{1}{2U^{\frac{1}{2}}}\frac{\mathrm{d}^2U}{\mathrm{d}x^2} - \frac{1}{4U^{\frac{3}{2}}}\left(\frac{\mathrm{d}U}{\mathrm{d}x}\right)^2\right] \end{aligned} \tag{B.3}$$

Multiplying both equations with $\mathcal{H}^{-1} = 1/(H_0 U^{\frac{1}{2}})$ yield the following:

$$\frac{1}{\mathcal{H}}\frac{\mathrm{d}\mathcal{H}}{\mathrm{d}x} = \frac{1}{2U}\frac{\mathrm{d}U}{\mathrm{d}x}, \tag{B.4}$$

and

$$\begin{aligned} \frac{1}{\mathcal{H}}\frac{\mathrm{d}^2\mathcal{H}}{\mathrm{d}x^2} &= \frac{1}{2U}\frac{\mathrm{d}^2U}{\mathrm{d}x^2} - \frac{1}{4U^2}\left(\frac{\mathrm{d}U}{\mathrm{d}x}\right)^2 \\ &= \frac{1}{2U}\frac{\mathrm{d}^2U}{\mathrm{d}x^2} - \left(\frac{1}{\mathcal{H}}\frac{\mathrm{d}U}{\mathrm{d}x}\right)^2 \end{aligned} \tag{B.5}$$

We now make the assumption that one of the density parameters dominate $\Omega_i >> \sum_{j\neq i}\Omega_i$, enabling the following approximation:

$$\begin{aligned} U &\approx \Omega_{i0} e^{-\alpha_i x} \\ \frac{\mathrm{d}^n U}{\mathrm{d}x^n} &\approx (-\alpha_i)^n \Omega_{i0} e^{-\alpha_i x}, \end{aligned} \tag{B.6}$$

from which we are able to construct:

$$\frac{1}{\mathcal{H}}\frac{\mathrm{d}\mathcal{H}}{\mathrm{d}x} \approx \frac{-\alpha_i \Omega_{i0} e^{-\alpha_i x}}{2\Omega_{i0} e^{-\alpha_i x}} = -\frac{\alpha_i}{2}, \tag{B.7}$$

and

$$\begin{aligned} \frac{1}{\mathcal{H}}\frac{\mathrm{d}^2\mathcal{H}}{\mathrm{d}x^2} &\approx \frac{\alpha_i^2 \Omega_{i0} e^{-\alpha_i x}}{2\Omega_{i0} e^{-\alpha_i x}} - \left(\frac{\alpha_i}{2}\right)^2 \\ &= \frac{\alpha_i^2}{2} - \frac{\alpha_i^2}{4} = \frac{\alpha_i^2}{4} \end{aligned} \tag{B.8}$$

which are quantities which should be constant in different regimes and we can easily check if our implementation of $\mathcal{H}$ is correct, which is exactly what we sought.

B.2. For η

TODO: fix this In order to test η we consider the definition, solve the integral and consider the same regimes as above, where one density parameter dominates:

$$\begin{aligned} \eta &= \int_{-\infty}^{x} \frac{c\mathrm{d}x}{\mathcal{H}} = \frac{-2c}{\alpha_i}\int_{x=-\infty}^{x=x} \frac{\mathrm{d}\mathcal{H}}{\mathcal{H}^2} \\ &= \frac{2c}{\alpha_i}\left(\frac{1}{\mathcal{H}(x)} - \frac{1}{\mathcal{H}(-\infty)}\right), \end{aligned} \tag{B.9}$$

where we have used that:

$$\begin{aligned} &\frac{\mathrm{d}\mathcal{H}}{\mathrm{d}x} = -\frac{\alpha_i}{2}\mathcal{H} \\ \implies &\mathrm{d}x = -\frac{2}{\alpha_i \mathcal{H}}\mathrm{d}\mathcal{H}. \end{aligned} \tag{B.10}$$

Since we consider regimes where one density parameter dominates, we have that $\mathcal{H}(x) \propto \sqrt{e^{-\alpha_i x}}$, meaning that we have:

$$\left(\frac{1}{\mathcal{H}(x)} - \frac{1}{\mathcal{H}(-\infty)}\right) \approx \begin{cases} \frac{1}{\mathcal{H}} & \alpha_i > 0 \\ -\infty & \alpha_i < 0. \end{cases} \tag{B.11}$$

Combining the above yields:

$$\frac{\eta\mathcal{H}}{c} \approx \begin{cases} \frac{2}{\alpha_i} & \alpha_i > 0 \\ \infty & \alpha_i < 0. \end{cases} \tag{B.12}$$

Notice the positive sign before ∞. This is due to α_i now being negative.